

ARTICLE TITLE: Wind-Induced Vibrations

AUTHORS NAME: Tracy Kijewski, Fred Haan, Ahsan Kareem

AUTHORS AFFILIATION: NatHaz Modeling Laboratory, Department of Civil Engineering and Geological Sciences, University of Notre Dame

AUTHOR ADDRESS: University of Notre Dame, 156 Fitzpatrick Hall, Notre Dame, IN, 46556 USA

## INTRODUCTION

As modern structures move toward taller and more flexible designs, the problems of wind effects on structures -- those compromising structural integrity and those inducing human discomfort-- have become increasingly apparent. To fully address this problem, a diverse collection of contributions must be considered, as illustrated in Figure 1. It is the complexity and uncertainty of the wind field and its interaction with structures that necessitates such an interdisciplinary approach, involving scientific fields such as meteorology, fluid dynamics, statistical theory of turbulence, structural dynamics, and probabilistic methods. The following sections will describe the contributions from each of these areas, beginning with a description of the wind field characteristics and the resulting wind loads on structures. Subsequent sections will then address procedures for determining wind-induced response, including traditional random vibration theory and code-based approximations, with an example to illustrate the application of both approaches. The treatment of wind effects on structures will conclude with a discussion of aeroelastic effects, wind tunnel testing, and the evolving numerical approaches. <insert Figure 1 near here>

## WIND CHARACTERISTICS

Civil engineering structures are immersed in the earth's atmospheric boundary layer, which is characterized by the earth's topographic features, e.g., surface roughness. The most common

description of the wind velocity within this boundary layer superimposes a mean wind component, described by a mean velocity profile, with a fluctuating velocity component. The vertical variation of the mean wind velocity,  $\bar{U}$ , can be represented by a logarithmic relationship, or by a power law given as:

$$\bar{U}(z) = \bar{U}_{ref} \left( \frac{z}{z_{ref}} \right)^a \quad (1)$$

where  $z_{ref}$  is the reference height,  $\bar{U}_{ref}$  is the mean reference velocity, and  $a$  is a constant that varies with the roughness of the terrain, with specific values defined in fundamental texts.

The fluctuating wind field is characterized by temporal averages, variances of velocity components, probabilities of exceedance, energy spectra, associated length scales, and space-time correlations. One important measure is the total energy of the wind fluctuations, expressed as the standard deviation of the velocity fluctuations normalized by the mean wind velocity, and referred to as *turbulence intensity*. The *energy spectra* describe the distribution of energy at each frequency, whereas the *space-time correlation* describes the degree to which velocity fluctuations are correlated in space and/or time. A measure of the average size of turbulent eddies, the *length scale*, can be then estimated by integrating velocity cross-correlation functions.

## WIND LOADS ON STRUCTURES

Just as the most elementary description of the velocity of the oncoming wind field superimposes a mean component,  $\bar{U}(z)$ , increasing with height according to the power law given in Eq. 1, with a randomly fluctuating component,  $u(z,t)$ , the oncoming wind will impose loads on the structure that vary both spatially and temporally. The fluctuating wind velocity translates directly

into fluctuating positive pressures ( $p_w(z, t)$ ) distributed across the building's windward face, as shown in Figure 2. Corresponding negative pressures,  $p_l(z, t)$ , result on the leeward face of the structure. <Figure 2 near here>

Upon impacting the windward face, the wind is then deflected around the structure and accelerated such that it cannot negotiate the sharp corners and thus separates from the building, leaving a region of high negative pressure, also shown in Figure 2. This separated flow forms a shear layer on each side, and subsequent interaction between the layers results in the formation of discrete vortices, which are shed alternately. This region is generally known as the *wake region*.

The three dimensional simultaneous loading of the structure due to its interaction with the wind results in three structural response components, illustrated in Figure 2. The first, termed the alongwind component, primarily results from pressure fluctuations in the approach flow, leading to a swaying of the structure in the direction of the wind. The acrosswind component constitutes a swaying motion perpendicular to the direction of the wind and are introduced by side-face pressure fluctuations primarily induced by the fluctuations in the separated shear layers, vortex shedding and wake flow fields. The final torsional component results from imbalances in the instantaneous pressure distribution on the building surfaces. These wind load effects are further amplified on asymmetric buildings as a consequence of inertial coupling in the building structural system.

As the wind pressures vary spatially over the face of the structure, there is the potential for regions of high localized pressures, of particular concern for the design of cladding systems;

however, it is their collective effect that results in the integral loads used for the design of the structural system, which will be of primary interest in this discussion.

Since the alongwind motion primarily results from the fluctuations in the approach flow, its load effects have been successfully estimated using quasi-steady and strip theories, which imply that the fluctuating pressure field is linearly related to the fluctuating velocity field at any level on the building. Although the alongwind response may also include interference effects due to the buffeting of the structure by the wake of upstream obstacles, it is the gust response due to the oncoming wind that is primarily considered. Thus, the aerodynamic loads,  $F(t)$ , considering only this component, are expressed in terms of velocity fluctuations as

$$F(t) = 1/2 \mathbf{r} A C_D (\bar{U} + u(t))^2 \approx 1/2 \mathbf{r} A C_D \bar{U}^2 + \mathbf{r} A C_D \bar{U} u(t) \quad (2)$$

in which  $\mathbf{r}$  = air density,  $A$  = projected area of the structure loaded by the wind, and  $C_D$  = drag coefficient. This expression is approximated by ignoring the generally small term containing the square of the fluctuating velocity.

The preceding expression implicitly assumes that the velocity fluctuations approaching a structure are fully correlated over the entirety of the structure. This assumption may be valid for very small structures, but fails to hold for structures with larger spatial dimensions and leads to overestimation of loads. In this case, the effect of imperfect correlation of wind fluctuations is introduced conveniently through an aerodynamic admittance function. As this loading scenario is described relatively easily in the frequency domain, Eq. 2 is accordingly transformed and the aerodynamic admittance,  $\mathbf{c}^2(f)$ , is introduced

$$S_F(f) = (\mathbf{r} C_D)^2 \mathbf{c}^2(f) S_u(f) \quad (3)$$

where  $S_F(f)$ ,  $S_u(f)$  = power spectral density (PSD) of wind loads and wind fluctuations, respectively. Ideally,  $c^2(f)$  not only represents the lack of correlation in the approach flow, but it also captures any departure from quasi-steady theory that may result from complex nonlinear interactions between the fluctuating wind and the structure. The transformation of wind velocity fluctuations to wind force fluctuations is illustrated in the frequency domain in Figure 3. For simple rectangular plates and prisms, both experimental and theoretical information concerning  $c^2(f)$  is available. For typical buildings that are aerodynamically bluff, one needs to resort to wind tunnel tests to directly obtain the PSD of the aerodynamic force. Alternatively, one can invoke the strip and quasi-steady theories with appropriate correlation structure of the approaching flow field to estimate  $c^2(f)$  and hence  $S_F(f)$ ; however, this may introduce some uncertainty in the estimates, as this approach may not fully capture all the features of the wind-structure interactions.

The approach described above has served as a building block for the “Gust Loading Factor” used in most building codes. However, the acrosswind and torsional responses cannot be treated in terms of these gust factors inasmuch as they are induced by the unsteady wake fluctuations, which cannot be conveniently expressed in terms of the incident turbulence. As a result, experimentally derived loading functions have been introduced. Accordingly, the acrosswind and torsional load spectra obtained by synthesizing the surface pressure fields on scale models of typical building shapes are available in literature. In a recent study, scale models of a variety of basic building configurations, with a range of aspect ratios, were exposed to simulated urban and suburban wind fields to obtain mode-generalized loads. These data are available through the authors’ interactive database at [www.nd.edu/~nathaz](http://www.nd.edu/~nathaz).

## WIND-INDUCED RESPONSE: THEORY

In order to derive the structural response from aerodynamic loads, basic random vibration theory is utilized. The equations of motion of a structure represented by a discretized lumped-mass system are given by

$$[\mathbf{M}]\{\ddot{x}(t)\} + [\mathbf{C}]\{\dot{x}(t)\} + [\mathbf{K}]\{x(t)\} = \{F(t)\} \quad (4)$$

in which  $\mathbf{M}$ ,  $\mathbf{C}$  and  $\mathbf{K}$  = assembled mass, damping and stiffness matrices of the discretized system, respectively,  $x$  is the displacement, and  $\dot{x}$  and  $\ddot{x}$  are the first two time derivatives of  $x$ , representing velocity and acceleration, respectively. In general, these equations are derived to provide two translations and one rotation per story level; however, for the sake of illustration, it is assumed here that the structure is uncoupled in each direction. By employing the standard transformation of coordinates, the following modal representation is obtained for one of the translation directions

$$\ddot{q}_j + 2\mathbf{z}_j(\mathbf{w}_n)_j \dot{q}_j + (\mathbf{w}_n)_j^2 q_j = P_j(t) \quad (5)$$

in which  $P_j(t) = \{\mathbf{f}_j\}^T \{F(t)\}$  where  $[\ ]^T$  denotes transpose,  $\mathbf{f}_j$ ,  $\mathbf{z}_j$  and  $(\mathbf{w}_n)_j = 2\mathbf{p}(f_n)_j$  are the  $j^{\text{th}}$  mode shape, modal critical damping ratio and natural frequency, respectively, and  $q$  and its derivatives now represent modal response quantities related to  $x$  and its derivatives, respectively, by  $\{x(t)\} = [\mathbf{f}_j] \{q_j(t)\}$ . The PSD of response,  $S_{q_j^{(r)}}$  is given by

$$S_{q_j^{(r)}}(f) = \left| H_j^{(r)}(i2\mathbf{p}f) \right|^2 S_{P_j}(f) \quad (6)$$

$$S_{P_j}(f) = \{\mathbf{f}_j\}^T [S_F(f)] \{\mathbf{f}_j\} \quad (7)$$

in which  $\left| H_j^{(r)}(i2\mathbf{p}f) \right|$  is  $j^{\text{th}}$ -mode frequency response function (FRF). The superscript  $r$  indicates the derivative of response, i.e.,  $r = 0,1,2,3$  denotes displacement, velocity, acceleration and jerk. Determination of wind-induced response by this approach is summarized in Figure 3. <insert Figure 3 near here>

The root mean square (RMS) value of response in physical coordinates,  $\mathbf{s}_{x^{(r)}}^2$ , is then given by the weighted superposition of all  $N$  modal contributions

$$\mathbf{s}_{x^{(r)}}^2 = \sum_{j=1}^N \frac{\mathbf{f}_j^2 \mathbf{p}(f_n)_j S_{P_j}(f_n)_j (2\mathbf{p}(f_n)_j)^{2r}}{4(2\mathbf{p}(f_n)_j)^4 \mathbf{z}_j m_j^2} + \sum_{j=1}^N \frac{\mathbf{f}_j^2 \int_0^{(f_n)_j} S_{P_j}(f) df (2\mathbf{p}(f_n)_j)^{2r}}{(2\mathbf{p}(f_n)_j)^4 m_j^2} \quad (8)$$

where  $m_j$  is the  $j^{\text{th}}$  modal mass,  $m_j = \{\mathbf{f}_j\}^T [\mathbf{M}]$ , and the first term of Eq. 8 represents the resonant component, and the second term, the background component. The preceding equation is an approximation of the area under the response PSD, which is very close to exact for most lightly damped structures.

## WIND-INDUCED RESPONSE: CODES & STANDARDS

International codes and standards have simplified the random vibration-based response analysis described in the previous section through the use of simplified algebraic expressions and the statistically derived gust effect factor, which accounts for the gustiness of the wind by providing equivalent static loads. Both time and spatial averaging play an important role in the development of gust factors, as does the site terrain, structure size and dynamic characteristics.

Through the use of random vibration theory, the dynamic amplification of loading or response, represented by the gust effect factor, can be readily defined. For example, the expected peak response  $y_{\max}^{(r)}$  can be estimated from the RMS value  $\mathbf{s}_{y^{(r)}}$  and mean value  $\bar{y}^{(r)}$  by the following expression, based on the probabilistic description of peak response during an interval  $T$

$$y_{\max}^{(r)} = \bar{y}^{(r)} + g^{(r)} \mathbf{s}_{y^{(r)}}. \quad (9)$$

The peak factor  $g^{(r)}$  varies between 3.5 and 4 and is given by

$$g = \sqrt{2 \ln((f_n)_1 T)} + 0.5772 / \sqrt{2 \ln((f_n)_1 T)}. \quad (10)$$

The gust effect factor (GEF)  $G$  is then defined as the ratio of the maximum expected response to the mean response:

$$G = \frac{y_{\max}^{(r)}}{\bar{y}^{(r)}} = 1 + g^{(r)} \frac{\mathbf{s}_{y^{(r)}}}{\bar{y}^{(r)}}. \quad (11)$$

The RMS response represents the area under the power spectral density of  $y^{(r)}$ , which can be described in terms of a background component  $Q$ , representing the response due to quasi-steady effects, and a resonant contribution  $R$  to account for dynamic amplification. To simplify the determination of these terms, international standards provide a series of simplified algebraic expressions. Typically  $G$  is defined in terms of the displacement response

$$G = 1 + 2g_{y^{(0)}} I_H \sqrt{Q + R} \quad (12)$$

where  $I_H$  = turbulence intensity at the top of the structure.  $Q$  and  $R$  respectively represent the contributions of the background and resonant components approximated in Eq. 8.

Most major codes and standards around the world account for the dynamic effects of wind in terms of the equivalent static loads  $F_{eq}$  through the use of the GEF

$$F_{eq}(z) = GC_{fx}\bar{q}(z)A \quad (13)$$

where the mean wind pressure is  $\bar{q} = 1/2\rho\bar{U}^2$  and  $C_{fx}$  = mean alongwind aerodynamic force coefficient. Each international standard uniquely defines  $G$  based on the form in Eq. 12. For example, in the ASCE 7-98 Standard the gust factor is defined as:

$$G = 0.925 \left( \frac{1 + 1.7I_{\bar{z}}\sqrt{g_Q^2Q^2 + g_R^2R^2}}{1 + 1.7g_vI_{\bar{z}}} \right) \quad (14)$$

where three peak factors are defined:  $g_Q$  and  $g_v$  are taken as 3.4 for simplicity and  $g_R$  is determined from Eq. 10 with  $T=3600$  sec, and  $I_{\bar{z}}$ , the turbulence intensity at the equivalent height of the structure,  $\bar{z}$ , is determined by a code-specified expression.

The background and resonant response components are similarly defined by approximate expressions

$$Q^2 = \frac{1}{1 + 0.63 \left( \frac{b+h}{L_{\bar{z}}} \right)^{0.63}} \quad (15)$$

$$R^2 = \frac{1}{b} R_n R_h R_b (0.53 + 0.47R_L) \quad (16)$$

where  $b$  and  $h$  are the width and height, respectively, of the structure, shown in Figure 2, and  $L_{\bar{z}}$  is the integral length scale of turbulence at the equivalent height. The resonant component involves 4 factors ( $R_n$ ,  $R_h$ ,  $R_b$ ,  $R_L$ ) which are dependent upon the first mode natural frequency, defined as  $n_1$  in ASCE 7-98, and damping ratio, defined in the standard as  $\mathbf{b}$ , as well as the dimensions of the structure, the mean wind speed at the equivalent height,  $\bar{V}_{\bar{z}}$ , and the wind field's characteristics. Expressions for these terms may be found in ASCE 7-98.

Following the determination of the gust effect factor, the maximum alongwind displacement  $X_{max}$  and RMS accelerations  $\mathbf{S}_{\ddot{x}}$  may be directly calculated

$$X_{\max}(z) = \frac{\mathbf{f}(z) \mathbf{r} b h C_{fx} \hat{V}_{\bar{z}}^2}{2m_1 (2\pi n_1)^2} K G \quad (17)$$

$$\mathbf{s}_{\ddot{x}}(z) = \frac{0.85 \mathbf{f}(z) \mathbf{r} b h C_{fx} \bar{V}_{\bar{z}}^2}{m_1} I_{\bar{z}} K R \quad (18)$$

where  $\hat{V}_{\bar{z}}$  is the three second gust at the equivalent height,  $\mathbf{f}(z)$  is assumed to be the fundamental mode shape,  $m_1$  is the first mode mass and  $K$  is a coefficient representative of the terms resulting from the integration of the mode shape and wind profile in the determination of the RMS response. Expressions for these terms are also provided in ASCE 7-98. Note that, in the case of the acceleration response, background effects are not considered, thus the gust effect factor is not directly used as defined in Eq. 14. It is instead replaced with a collection of terms analogous to using a gust effect factor with only a resonant component.

## WIND-INDUCED RESPONSE: EXAMPLE

To illustrate the determination of wind-induced response by both random vibration theory and by the code-based procedure, the following example is provided. Table 1 lists the assumed properties of the structure, which is located in a city center. The basic wind speed, measured as a 3 second gust, at the reference height of 33 ft (10 m) in open terrain, is taken as 90 mph (40.23 m/s). For the sake of brevity, only acceleration response will be provided, considering only the first mode with an assumed linear mode shape. To further simplify the analysis, the response will be calculated only at the structure's full height, at which point the mode shape given in Table 1 would equal unity. <insert Table 1 near here>

The RMS accelerations in the alongwind direction were first determined in accordance with ASCE 7-98, by Eq. 18, with all calculated parameters listed in Table 2. Unfortunately, as discussed previously, acrosswind and torsional responses cannot be determined by the same analytical procedure and are thus omitted from the ASCE 7 Standard. However, these response components, as well as the alongwind response, can readily be determined by Eq. 8 with the aid of the wind tunnel data provided in Figure 4. Note that it is common practice to plot these load spectra in a non-dimensional form,  $S^*$ , as defined in Figure 4, where  $\bar{U}_H$  is the mean wind velocity at the height of the building, in urban terrain. A power law relationship (Eq. 1) can be used to translate the reference wind velocity of 90 mph from open terrain at 33 ft (10 m) to urban terrain at the building height. <insert Table 2 and Figure 4 near here>

In the case of acceleration response,  $r=2$  and  $N=1$  in Eq. 8, as only first mode contributions are considered. Note also that in Eq. 8,  $m_j$  is defined as the modal mass for the alongwind and acrosswind directions, taken as the total mass of the building, divided by 3; however, for the

torsional response, this modal mass term must be replaced by the first mode mass moment of inertia determined by:  $\frac{1}{12}m_1(b^2 + d^2)$ , where  $d$  is the depth of the structure as shown in Figure

2. In addition, the torsional analysis requires the multiplication of the spectral density by a reduction factor to account for the assumption of a constant mode shape inherent in force-balance experimental measurements.

Examining first the properties in Table 2, a comparison of  $R^2$  and  $Q^2$  reveals that this particular structure receives nearly equal contributions from the background and resonant components. For the alongwind response, shown in Table 3, the simplified response estimate given by ASCE 7-98 compares well with the wind tunnel data. Also note that the acrosswind accelerations are twice that of the alongwind response, illustrating that acrosswind response components have a greater role in determining the habitability performance of a structure. On the other hand, the structure's torsional response is slightly less than the alongwind, which should be no surprise considering that the structure has no geometric or structural asymmetries and that the loading data from the wind tunnel was obtained using an isolated building model. <insert Table 3 near here>

## SPECIAL TOPICS: AEROELASTIC EFFECTS

The determination of wind-induced loads and response discussed previously did not account for aeroelastic effects, which can sometimes have significant contributions to the structural response. Response deformations can alter the aerodynamic forces, thus setting up an interaction between the elastic response and aerodynamic forces commonly referred to as *aeroelasticity*. Aeroelastic contributions to the overall aerodynamic loading are distinguished from other unsteady loads by recognizing that aeroelastic loads vanish when there is no structural motion. Different types of

aeroelastic effects are commonly distinguished from each other. They include vortex-induced vibration, galloping, flutter, and aerodynamic damping.

As alluded to earlier, aerodynamically bluff cross sections shed vortices at a frequency governed by the non-dimensional *Strouhal number*,  $St$  :

$$St = \frac{f_s b}{U} \quad (19)$$

where  $f_s$  is the shedding frequency (in Hz). The shedding of vortices generates a periodic variation in the pressure over the surface of the structure. When the frequency of this variation approaches one of the natural frequencies of a structure, vortex-induced vibration can occur. The magnitudes of these vibrations are governed both by the structure's inherent damping characteristics and by the mass ratio between the structure and the fluid it displaces. These two effects are often combined in the *Scruton number* defined as:

$$Sc = \frac{4\rho z m}{r b^2} \quad (20)$$

where  $m$  is the mass per unit length of the structure.

Vortex-induced vibration is more complex than a mere resonant forcing problem. Nonlinear interaction between the body motion and its wake results in the “locking in” of the wake to the body's oscillation frequency over a larger velocity range than would be predicted using the Strouhal number. Vortex-induced vibration, therefore, occurs over a range of velocities that increases as the structural damping decreases.

*Galloping* occurs for structures of certain cross sections at frequencies below those of vortex-induced vibration. One widely known example of galloping is the large across-wind amplitudes exhibited by power lines when freezing rain has resulted in a change of their cross section. Analytically, galloping is considered a “quasi-steady” phenomenon because knowledge of the static aerodynamic coefficients of a given structure (i.e., mean lift and drag forces on a stationary model) allows quite reliable prediction of galloping behavior.

Stability of aeroelastic interactions is of crucial importance. The attenuation of structural oscillations by both structural and aerodynamic damping characterizes stable flow-structure interactions. In an unstable scenario, the motion-induced loading is further reinforced by the body motion, possibly leading to catastrophic failure. Such unstable interactions involve extraction of energy from the fluid flow such that aerodynamic effects cancel structural damping. *Flutter* is the term given to this unstable situation, which is a common design issue for long span bridges.

Depending on the phase of the force with respect to the motion, self-excited forces can be associated with the displacement, the velocity, or the acceleration of the structure. Because of these associations, these forces can be thought of as “aerodynamic contributions” to stiffness, damping, and mass, respectively. In addition to stiffness and damping, aeroelastic effects can couple modes that are not coupled structurally. Whenever the combined aeroelastic action on various modes results in negative damping for a given mode, flutter occurs. By means of structural dynamics considerations and aerodynamic tailoring, flutter must be avoided for the wind velocity range of interest. Even without resulting in flutter, aeroelastic effects can have a significant effect on response.

## SPECIAL TOPICS: WIND TUNNEL TESTING

Despite the obvious advances of computational capabilities over the years, the complexity of the bluff body fluid-structure interaction problems concerning civil engineering structures has precluded numerical solutions for the flow around structures. Thus, wind tunnels remain, at this juncture, the most effective means of estimating wind effects on structures. However, it should be noted that not all structures require wind tunnel testing. For many conventional structures, for example, low-rise buildings, code-based estimates may well suffice. Wind tunnel testing may be necessary, however, when dealing with a novel design or a design for which dynamic and aeroelastic effects are difficult to anticipate. Examples of such structures include, but are not limited to, long-span bridges and tall buildings.

Wind tunnel testing of a given structure first involves appropriate modeling of the wind environment, necessitating various scaling considerations. Geometric scaling is based on the boundary layer height, the scale of turbulence, and the scale of the surface roughness all constrained by the size of the wind tunnel itself. Ideally, these lengths should hold to the same scaling ratio—a performance that can be approached when the boundary layer is simulated over a long fetch with scaled floor roughness. Dynamic scaling requires Reynolds number equality between the wind tunnel and the prototype. Without extraordinary measures, this is most often not possible and must be kept in mind when interpreting results. Velocity scaling is most often obtained from elastic forces of the structure and inertial forces of the flow. Kinematic scaling involves appropriate distributions of the mean velocity and turbulence intensity and can be achieved with flow manipulation in the wind tunnel.

Both active and passive means are available for generating turbulent boundary layers. While active devices such as air jets, flapping vanes and airfoils are capable of generating a wide range of turbulence parameters, passive devices are cheaper and more efficient to implement. Passive devices include spires, fences, grids, and floor roughness. Depending on the length and cross sectional size of the tunnel, surrounding terrain may be modeled as well.

Once an appropriate incident flow has been generated, there are several options for obtaining aerodynamic load data for the structure of interest. Pressure measurements can be performed on the surface of a model, forces can be quantified from the base of a lightweight, rigid model, or forces can be obtained from an aeroelastic model of the structure. Pressure measurements are capable of quantifying localized loading on a structure's surface. Issues such as fatigue loads for cladding panels and panel anchor and glass failure require such localized analysis.

Integrated loads on a structure are often estimated with high-frequency base balances. These devices are generally integrated into a rotating section of the floor of a wind tunnel. A lightweight model of the structure is mounted on the balance for measuring wind loads over a range of incidence angles. The low mass of the model is necessary to ensure that the natural frequency of the model-balance system is well above any expected wind forcing frequency. A primary advantage of this approach is that modal force spectra are obtained directly and can be used in subsequent analytical estimations of building response. As long as the structural geometry does not change, the forces can be used to analyze the effects of internal structural design changes without the need for further wind tunnel tests.

Aeroelastic models allow interaction between structural motion and aerodynamic forces. Such models can be constructed as continuous or discrete models. Continuous models require

specialized materials having structural properties matching those of the prototype. Discrete models are simpler to implement and consist of an internal spine to account for structural dynamic features with an external cladding that maintains proper geometric scaling with the prototype. Dynamic response of both buildings and bridges can be estimated utilizing such models.

## SPECIAL TOPICS: NUMERICAL METHODS

With the evolution of computer capabilities, numerical methods have presented another option for the analysis of fluid-structure interactions. A host of simulation schemes to generate wind fields and the associated response, in a probabilistic framework, are currently available. However, these schemes rely on quasi-steady formulations to transform wind fluctuations into load fluctuations. A welcome departure from the limitations of such approaches is offered by the field of Computational Fluid Dynamics (CFD), serving as a promising alternative to wind tunnel testing. One of the more attractive approaches within this area involves the solution of the Navier-Stokes equations in the Large Eddy Simulation (LES) framework to simulate pressure fields around structures that convincingly reproduce the experimentally measured pressure-distributions in both the mean and RMS, as well as replicating the aerodynamic forces and flow re-attachment features. Coupled with computer-aided flow visualization, which provides visual animation, this numerical simulation may serve as a useful tool to analyze the evolution of flow fields around structures and estimate the attendant loads. This approach definitely has merit, and as computational capacity increases, these schemes will eventually become the methods of choice.

## FURTHER READING

American Society of Civil Engineers, 1999, *Minimum Design Loads for Buildings and Other Structures*, ASCE7-98. Reston, VA.

Cermak, J.E., 1976, "Aerodynamics of Buildings," *Annual Review of Fluid Mechanics*, Vol. 8.

Cermak, J.E., 1987, "Advances in Physical Modeling for Wind Engineering," *Journal of Engineering Mechanics*, Vol. 113, No. 5, pp. 737-756.

Kareem, A., 1987, "Wind Effects on Structures: A Probabilistic Viewpoint," *Probabilistic Engineering Mechanics*, Vol. 2, No. 4, pp. 166-200.

Kareem, A., Kijewski, T. and Tamura, Y., (1999), "Mitigation of Motions of Tall Buildings with Specific Examples of Recent Applications," *Wind & Structures*, Vol. 2, No. 3, pp. 201-251.

Kijewski, T. and Kareem, A., 1998, "Dynamic Wind Effects: A Comparative Study of Provisions in Codes and Standards with Wind Tunnel Data," *Wind & Structures*, Vol. 1, No. 1, pp. 77-109.

Lutes, L.D. and Sarkani, S., 1997, *Stochastic Analysis of Structural and Mechanical Vibrations*. Prentice Hall, New Jersey.

Murakami, S., 1998, "Overview of Turbulence Models Applied in CWE-1997," *Journal of Wind Engineering and Industrial Aerodynamics*, Vols. 74-76, pp. 1-24.

Simiu, E. and Scanlan, R., 1996, *Wind Effects on Structures*. 3<sup>rd</sup> Ed., John Wiley and Sons, New York.

Solari, G. and Kareem, A., 1998, "On the Formulation of ASCE7-95 Gust Effect Factor," *Journal of Wind Engineering & Industrial Aerodynamics*, vol. 77 and 78, pp. 673-684.

Sutro, D., 2000, "Into the Tunnel," *Civil Engineering Magazine*, June, pp. 37-41.

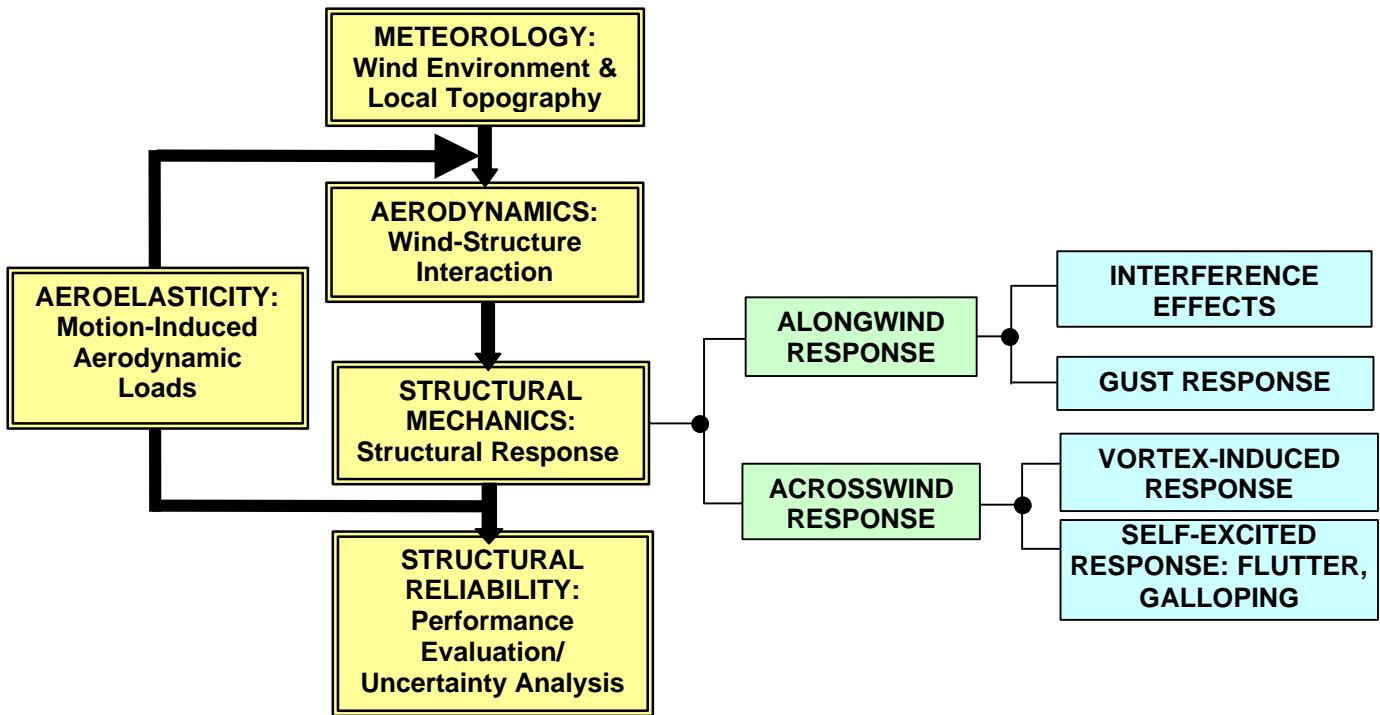


Figure 1: Overview of scheme to determine wind effects on structures.

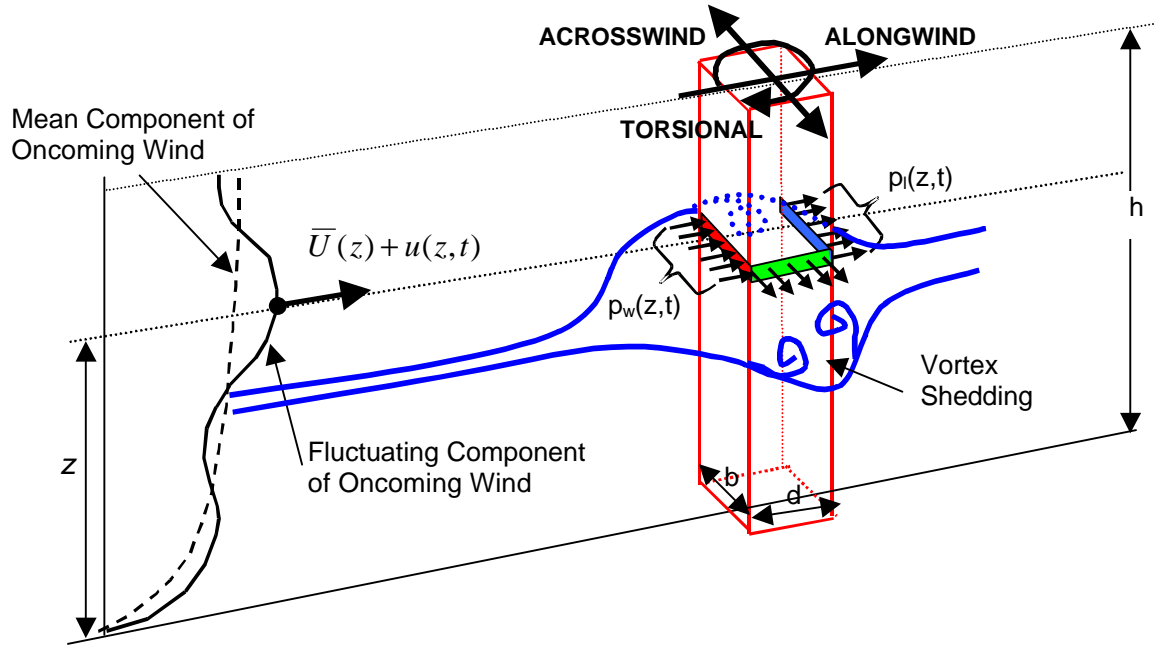


Figure 2: Description of oncoming wind field and resulting wind-induced effects on structure.

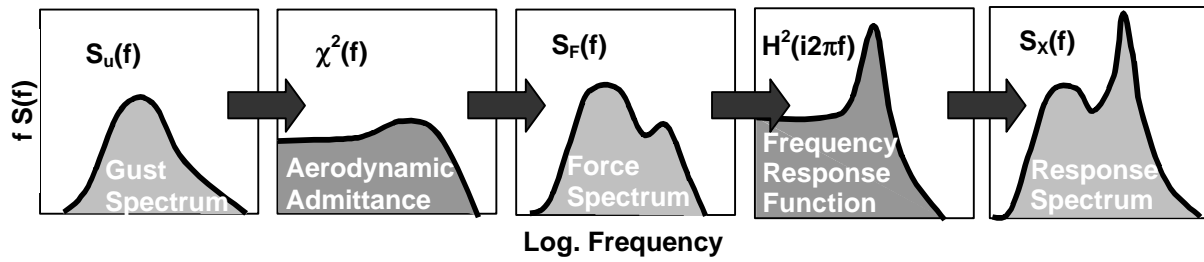


Figure 3: Procedure for determination of response spectrum.

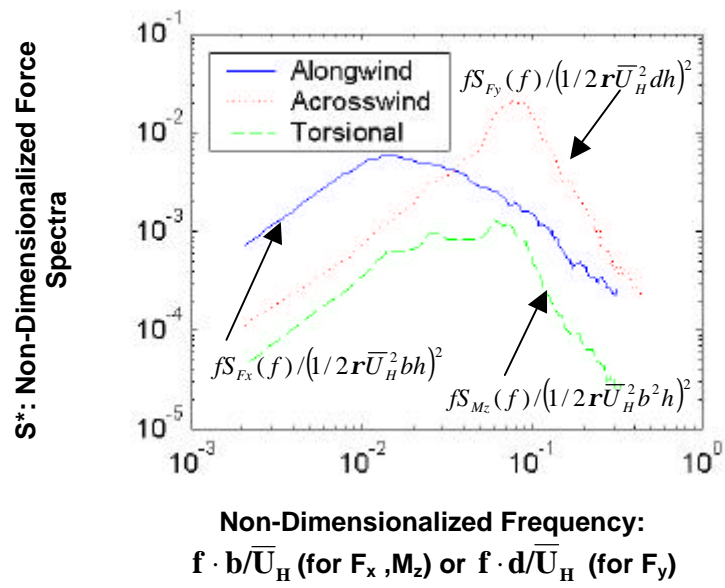


Figure 4: Aerodynamic load spectra obtained via force-balance tests in a wind tunnel.

---

Table 1: Assumed structural properties.

---

$h$	600 ft (182.88 m)
$b$	100 ft (30.48 m)
$d$	100 ft (30.48 m)
$r$	0.0024 slugs/ft <sup>3</sup> (1.25 kg/m <sup>3</sup> )
$C_{fx}$	1.3
$(f_n)_1$ : alongwind, acrosswind, torsion	0.2 Hz, 0.2 Hz , 0.35 Hz
$r_B$ : building density	12 lb/ft <sup>3</sup> = 0.3727 slugs/ft <sup>3</sup> (192.22 kg/m <sup>3</sup> )
$b$	0.01
First Mode Shape	$f(z)=(z/H)$

---

Table 2: Values Calculated from ASCE 7-98.

$I_{\bar{z}}$	0.302
$L_{\bar{z}}$	594.52 ft
$Q^2$	0.589
$R_n$	0.111
$R_h$	0.146
$R_b$	0.555
$R_L$	0.245
$R^2$	0.580
$g_Q, g_v$	3.4 (assumed)
$g_R$	3.787
$G$	1.01
$K$	0.502
$m_I$	745,400 slugs (10,886,129 kg)
$\bar{V}_{\bar{z}}$	87.83 ft/s (26.77 m/s)
$U_H$	102.36 ft/s (31.20 m/s)
$S_{F_x}^*(n_1)^a$	0.00048
$S_{F_y}^*(n_1)^a$	0.0023
$S_{M_z}^*(n_1)^{a,b}$	0.000025

<sup>a</sup>Spectral values in non-dimensional form. See Figure 4.

<sup>b</sup> $S_{M_z}(n_1)$  should be multiplied by a correction factor of 0.7042.

Table 3: Calculated RMS Lateral Accelerations (in milli-g's).

	Alongwind	Acrosswind	Torsional <sup>a</sup>
ASCE 7-98 (Eq. 18)	5.90	N/A	N/A
Experimental (Eq. 8)	6.17	13.5	5.05

<sup>a</sup>Torsion-induced lateral accelerations at building corner.

---

NOTATION

---

$A$	<i>projected area of building exposed to wind</i>
$\alpha$	<i>power law exponent</i>
$b$	<i>width of structure</i>
$\beta$	<i>critical damping ratio (ASCE 7-98)</i>
$C$	<i>structural damping matrix</i>
$C_{fx}$	<i>alongwind aerodynamic force coefficient</i>
$C_D$	<i>drag coefficient</i>
$d$	<i>depth of structure</i>
$c^2$	<i>aerodynamic admittance function</i>
$f$	<i>frequency</i>
$f_n$	<i>natural frequency in Hertz</i>
$f_s$	<i>vortex shedding frequency in Hertz</i>
$F$	<i>force (or load), in physical coordinates</i>
$F_{eq}$	<i>equivalent static load</i>
$g$	<i>peak factor</i>
$G$	<i>gust effect factor</i>
$\phi$	<i>mode shape</i>
$h$	<i>height of structure</i>
$H$	<i>frequency response function</i>
$I_H$	<i>turbulence intensity at top of structure</i>
$I_{\bar{z}}$	<i>turbulence intensity at equivalent height</i>
$j$	<i>subscript denoting modal index</i>

$K$	<i>integration constant (ASCE 7-98)</i>
$K$	<i>structural stiffness matrix</i>
$L_z$	<i>integral length scale of turbulence at equivalent height</i>
$M$	<i>structural mass matrix</i>
$m$	<i>structural mass per unit height</i>
$m_j$	<i><math>j^{\text{th}}</math> modal mass</i>
$n_1$	<i>fundamental natural frequency (ASCE 7-98)</i>
$N$	<i>total number of modal components</i>
$P$	<i>force (or load), in modal coordinates</i>
$p_l$	<i>wind pressure on leeward face of building</i>
$p_w$	<i>wind pressure on windward face of building</i>
$Q$	<i>background component</i>
$\bar{q}$	<i>mean wind pressure</i>
$q$	<i>modal displacement</i>
$\dot{q}$	<i>modal velocity</i>
$\ddot{q}$	<i>modal acceleration</i>
$r$	<i>superscript denoting derivative order</i>
$R$	<i>resonant component</i>
$R_n, R_h, R_b, R_L$	<i>terms for approximation of resonant component (ASCE 7-98)</i>
$\rho$	<i>air density</i>
$\rho_b$	<i>building density</i>

$Sc$	<i>Scruton Number</i>
$S_F$	<i>power spectral density of wind loads, in physical coordinates</i>
$S_p$	<i>power spectral density of wind loads, in modal coordinates</i>
$S_q$	<i>power spectral density of response, in modal coordinates</i>
$St$	<i>Strouhal Number</i>
$S_u$	<i>power spectral density of wind fluctuations</i>
$S^*$	<i>non-dimensionalized load spectra</i>
$\sigma$	<i>root mean square</i>
$t$	<i>time</i>
$T$	<i>time interval</i>
$u$	<i>longitudinal velocity fluctuations</i>
$\bar{U}$	<i>mean wind velocity</i>
$\bar{U}_{ref}$	<i>mean wind velocity at reference height</i>
$\bar{U}_H$	<i>wind velocity at building height</i>
$\bar{V}_{\bar{z}}$	<i>mean wind velocity at equivalent height</i>
$\hat{V}_{\bar{z}}$	<i>3 second gust at equivalent height</i>
$x$	<i>structural displacement, in physical coordinates</i>
$\dot{x}$	<i>structural velocity, in physical coordinates</i>
$\ddot{x}$	<i>structural acceleration, in physical coordinates</i>
$X_{max}$	<i>maximum alongwind displacement (ASCE 7-98)</i>
$\omega_n$	<i>natural frequency in rad/sec</i>
$\bar{y}$	<i>mean response</i>
$y_{max}$	<i>expected peak response</i>
$z$	<i>vertical position</i>
$\bar{z}$	<i>equivalent height</i>
$z_{ref}$	<i>reference height</i>
$\zeta$	<i>critical damping ratio</i>

$[\ ]^T$

*transpose operator*